1730 *Macromolecules* **2010**, *43*, 1730–1738
DOI: 10.1021/ma901924n

Macromolecules
ARTICLE

Reversible Addition−Fragmentation Chain Transfer in Microemulsions: Effect of Chain Transfer Agent Aqueous Solubility

Jennifer O'Donnell* and Eric W. Kaler

Center for Molecular and Engineering Thermodynamics, Department of Chemical Engineering, University of Delaware, Newark, Delaware 19716

Received August 30, 2009; Revised Manuscript Received December 15, 2009

ABSTRACT: Microemulsion polymerizations are attractive for investigating compartmentalization effects in heterogeneous reversible addition−fragmentation chain transfer (RAFT) polymerizations because the propagating radicals are segregated into surfactant stabilized polymer particles, which drastically reduces the effects of biradical termination. Also, microemulsion polymerizations do not involve the large monomer droplets that are present in emulsion and miniemulsion polymerizations. RAFT microemulsion polymerizations of butyl acrylate with a high water solubility chain transfer agent, methyl-2-(*O*-ethylxanthyl)propionate (MOEP), and a low water solubility chain transfer agent, methyl-2-(*O*-dodecylxanthyl)propionate (MODP), were investigated to determine the effect of chain transfer agent compartmentalization on the control of the polymerization. The partitioning of the chain transfer agent into the polymer particles is shown to be the primary factor in determining the final properties of the polymer and latex. Polymerizations with the high water solubility chain transfer agent MOEP produced stable latex nanoparticles (20−30 nm in diameter) containing low polydispersity poly(butyl acrylate) of predetermined molecular weight, whereas polymerizations with the low water solubility chain transfer agent MODP produced stable latex nanoparticles containing polymers with a multimodal molecular weight distribution.

Introduction

Reversible addition−fragmentation chain transfer (RAFT) is a robust method for controlling homogeneous free radical polymerizations to produce polymers with predetermined molecular weight, low polydispersity, and novel architectures.[1−3] However, incorporating RAFT into heterogeneous polymerizations (such as emulsion or miniemulsion) frequently leads to poor control of molecular weight, high polydispersity, and loss of colloidal stability.[4,5] Additionally, rate retardation is often more significant in heterogeneous polymerizations than in homogeneous polymerizations.[5] The increase in rate retardation in miniemulsions relative to bulk has been shown to result from compartmentalization effects[6] and increased radical exit from the polymerizing particles.[7] Similar compartmentalization effects have also been observed for atom transfer radical polymerizations (ATRP)[8−11] and nitroxide-mediated polymerization (NMP)[12−17] in heterogeneous media. Microemulsions are an attractive alternative to other types of heterogeneous polymerizations for both studying the RAFT reaction mechanism and incorporating RAFT to produce stable latex nanoparticles containing polymer chains of controlled molecular weight.[18] The advantages of microemulsions lie in the absence of monomer droplets and the high concentration of monomer-swollen micelles relative to polymer particles. The relatively low number of polymerizing particles minimizes the probability of a radical entering a particle and terminating. Therefore, the effect of the compartmentalization of the chain transfer agent can be studied in a simplified kinetic scheme by varying the aqueous solubility of the chain transfer agent. The primary disadvantages of microemulsion polymerization are the high ratio of surfactant to monomer necessary to stabilize the initial microemulsion and the low solids content of the final polymer latex.

The proposed mechanism of RAFT *microemulsion* polymerization, based on the original RAFT reaction mechanism proposed by Chiefari et al.,[1] is shown in Figure 1. Monomer (M) and chain transfer agent (XR) in excess of their respective solubility thresholds partition into micelles (Figure 1.1). Polymerization commences when a water-soluble initiator (I) decomposes and reacts with the monomer solubilized in the aqueous domain to form a propagating polymer ($P^{\bullet}$) (Figure 1.2). Upon reaching a critical degree of polymerization, the propagating radical is no longer soluble in the aqueous domain and enters a monomer-swollen micelle, thus initiating a polymer particle. Propagation continues in the polymer particle with monomer and chain transfer agent diffusing from surrounding uninitiated micelles to the locus of polymerization (Figure 1.3). The diffusion of chain transfer agent from the micelles to the polymer particles is necessary for complete activation of the chain transfer agent and the production of polymers with the desired molecular weight. However, the continuous diffusion of the chain transfer agent from the micelles to the polymer particles can also have the unwanted effect of increasing the breadth of the chain transfer agent per particle ratio distribution, which means that in a RAFT microemulsion polymerization the polymer particles may experience a broad range of reaction conditions.

After entering a polymer particle, the propagating radical ($P_n^{\bullet}$) reacts with a chain transfer agent (XR) to form a RAFT radical ($P_nX^{\bullet}R$). Subsequently, the RAFT radical cleaves to give a dormant polymer (XP_n) and a new radical ($R^{\bullet}$) (Figure 1.4). The new $R^{\bullet}$ radical reacts with monomer to initiate a new polymer ($P^{\bullet}$) within the same particle (Figure 1.5). Once an active polymer ($P^{\bullet}$) and one or more dormant polymers (XP_n) are present within one particle, an equilibrium is formed in which the polymers alternate between the dormant and active states.

*To whom correspondence should be addressed at Department of Chemical and Biological Engineering, 2033 Sweeney Hall, Iowa State University, Ames, IA 50011. Phone 515-294-1891; e-mail jodonnll@iastate.edu.

 Published on Web 01/25/2010

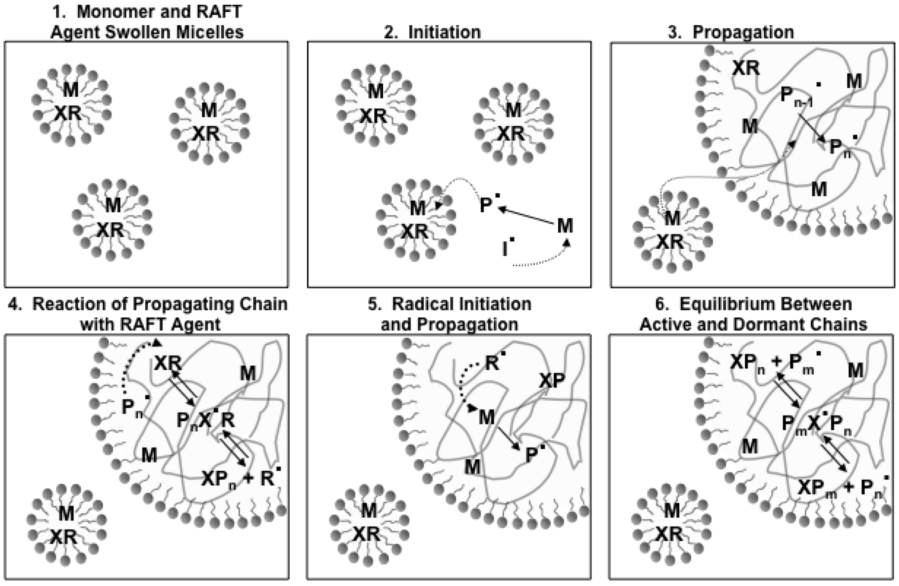

Figure 1. Proposed RAFT microemulsion polymerization mechanism: 1. Monomer (M) and chain transfer agent (XR) swollen micelles. 2. Initiation of a propagating polymer ($P^{\bullet}$) and entry into a micelle, which forms a polymer particle. 3. Diffusion of M and XR to the locus of polymerization. 4. Activation of the chain transfer agent to form a dormant polymer (XP) and a radical R group ($R^{\bullet}$). 5. Initiation of a new polymer within the same particle. 6. Equilibrium between active ($P^{\bullet}$) and dormant (XP) polymers.

The final latex dispersion consists of empty micelles and surfactant stabilized polymer particles in which the number of polymer molecules depends on the concentration of the chain transfer agent (Figure 1.6).

The present work incorporates the high water solubility chain transfer agent methyl-2-(*O*-ethylxanthyl)propionate (MOEP) and the low water solubility chain transfer agent methyl-2-(*O*-dodecylxanthyl)propionate (MODP) to control microemulsion polymerizations of butyl acrylate (BA). Small-angle neutron scattering studies have shown that monomers with a water solubility as low as 0.4 mM partition linearly between the micelles and polymer particles throughout the polymerization.[19] The water solubility of MOEP is 1.0 mM, so all of the MOEP is expected to diffuse from the micelles into the polymer particles during the polymerization. The facile diffusion of MOEP between the micelles and polymer particles is expected to lead to activation of all of the MOEP and the production of polymers with the desired molecular weight. The water solubility of MODP, on the contrary, is very low (< 0.01 mM) so the diffusion of MODP from the micelles to the polymer particles is expected to be slow. If the polymerization is completed before all of the MODP diffuses into the polymer particles, then these polymerizations will produce polymers with a molecular weight that is greater than the desired molecular weight.

Experimental Section

Materials. Dodecyltrimethylammonium bromide (DTAB) from TCI America and the initiator 2,2′-azobis[2-(2-imidazolin-2-yl)propane] dihydrochloride (VA-044) from Wako Pure Chemical Industries were used as received. *n*-Butyl acrylate (BA) from Aldrich was distilled under vacuum to remove the inhibitor and stored at 2 °C for less than 1 week prior to use. The RAFT agent methyl-2-(*O*-ethylxanthyl)propionate (MOEP) was provided by Rhodia and used as received. The MOEP purity was confirmed by ^{1}H NMR. δ: 1.35 (t, 3H, CH_3−CH$_2$), 1.51 (d, 3H, CH_3−C(COO)S), 3.69 (s, 3H, CH_3−OCO), 4.32 (q, 1H, CH−S(COO)CH$_3$), 4.56 (q, 2H, OCH_2−CH$_3$).

The RAFT agent methyl-2-(*O*-dodecylxanthyl)propionate (MODP) was synthesized with chemicals purchased from Aldrich. 1-Dodecanol and carbon disulfide were combined at a 1:1 molar ratio in dimethylformamide. The solution was cooled to 0 °C in an ice bath, and a 60 wt % solution of sodium hydride in mineral oil was added dropwise for a final 1-dodecanol to sodium hydride molar ratio of 1.0:1.1. The solution was warmed to room temperature and stirred for 30 min. Then the solution was cooled to 0 °C in an ice bath, and methyl-2-bromopropanoate was added at 10% molar excess with respect to 1-dodecanol. The solution was stirred for 30 min, then warmed to room temperature, and stirred for an additional 45 min. The product was extracted into ether, washed with an aqueous sodium chloride solution, and washed with water. The product was dried over magnesium sulfate, and the solvent was evaporated under vacuum. The purity of MODP was confirmed by ^{1}H NMR. δ: 0.81 (t, 3H, CH_3−CH$_2$), 1.19 (broad, 20H, CH_2−CH$_2$), 1.51 (d, 3H, CH_3−C(COO)S), 3.69 (s, 3H, CH_3−OCO), 4.32 (q, 1H, CH−S(COO)CH$_3$), 4.5 (q, 2H, OCH_2−CH$_3$).

Polymerizations. Microemulsions of BA in water stabilized by DTAB were prepared at $\alpha = 5.0$ and $\gamma = 12.0$, where $\alpha = \text{mass}_{oil}/(\text{mass}_{oil} + \text{mass}_{water}) \times 100$ and $\gamma = \text{mass}_{surfactant}/(\text{mass}_{surfactant} + \text{mass}_{oil} + \text{mass}_{water}) \times 100$. The surfactant was added to either a Mettler Toledo RC1 reactor (for calorimetric studies) or a jacketed 500 mL glass reactor (for gravimetric studies), and the reactor was purged with argon for 30 min. Degassed water was then added, and the temperature of the solution was increased to 45 °C. In the RC1, the heat capacity of the surfactant solution was measured at the reaction temperature using standard WinRC1 software. MOEP or MODP was combined with BA, sparged with argon, and added to the reactor. The temperature was allowed to equilibrate, and polymerization was initiated by injecting 2 mL of a sparged aqueous solution of VA044 into the reactor for a total VA044 concentration of 3.0 mM. For gravimetric analysis, samples were drawn from the reactor throughout the polymerization and rapidly frozen in liquid nitrogen to terminate the polymerization. For calorimetric studies, the heat of reaction was measured throughout the polymerization, and when the polymerization was complete, the heat capacity of the latex was measured. The conversion of the monomer as a function of time was then calculated from the heat evolved during the polymerization using standard WinRC1 software. Polymerizations were performed at chain transfer agent molecule per micelle ratios of 0.3, 0.6, 1.2, 2.4, 3.7, and 4.9. These chain transfer agent molecule per micelle ratios correspond to chain transfer agent concentrations of 1.3, 2.5, 4.6, 9.2, 14.5, and 19.0 mM. The chain transfer agent

per micelle ratio is calculated using the known volume of the monomer (V_{BA} = 239.2 Å^3) and the volume (V_{tail} = 350.2 Å^3)[20] and the area per headgroup (A_{head} = 68.0 Å^2)[20] of the surfactant.[21]

Gel Permeation Chromatography. Polymer samples collected during the gravimetric studies were dried under an air flow, washed with acetone to remove excess monomer, and dried at 50 °C in a vacuum oven overnight. To remove the surfactant, the dried samples were dissolved in tetrahydrofuran (THF), the solution was centrifuged, and the supernatant containing the polymer was decanted. After three cycles of suspending the surfactant pellet in fresh THF and centrifuging, the combined supernatants were dried and the polymer was dissolved in THF at a polymer weight fraction of 0.002. Gel permeation chromatography (GPC) analyses were performed on a Waters Alliance HPLC with UV and RI detection. Three Styragel columns were used in series: HR1 (100−5000 g/mol), HR4 (5000−500 000 g/mol), and HR6 (> 500 000 g/mol). Molecular weights were determined as poly(methyl methacrylate) equivalents and converted to apparent number-average molecular weights using the Mark−Houwink−Sakurada equation with $K_{BA} = 12.2 \times 10^{-5}$ dL/g, $a_{BA} = 0.700$, $K_{MMA} = 9.44 \times 10^{-5}$ dL/g, and $a_{MMA} = 0.719$.[22,23]

Quasi-Elastic Light Scattering. Latex solutions were diluted so that the surfactant concentration was 10 times the critical micelle concentration of DTAB (cmc = 16 mM). Quasi-elastic light scattering experiments were performed using a Brookhaven Instruments BI-200SM goniometer and laser light scattering system with a BI9000 digital correlator. The scattering angle was fixed at 90° and samples thermostated at 25 °C were irradiated with 488 nm light produced from a Lexel 2 W argon ion laser. Intensity correlation data were measured four times for each sample and fit with Brookhaven software using both a quadratic cumulants fit and the method of CONTIN. The allowable range of particle diameters for CONTIN fits was constrained between 5 and 50 nm, as this range consistently provided root-mean-square errors of less than 10^{-3} and agreement with the average particle diameter from the quadratic cumulants fit. The presented data are the result of averaging the volume-weighted particle size distribution of four runs.

Results and Discussion

Molecular Weight and Polydispersity. Apparent poly(butyl acrylate) number-average molecular weights (M_N) have been calculated from gel permeation chromatography (GPC) experiments using refractive index detection and narrow poly(methyl methacrylate) standards. The calculation of apparent molecular weights from the Mark−Houwink−Sakurada equation inherently introduces deviations between the apparent molecular weight and the true molecular weight.[24] In the present work, the apparent molecular weight distribution is calculated to be as much as 8% greater than the true molecular weight.[24] In addition, the reported polydispersity is slightly greater for the apparent molecular weight distribution than for the true molecular weight distribution. These predicted deviations from the true molecular weight distribution are expected to have a minimal effect on the trend of the number-average molecular weight as a function of conversion; however, quantitative analysis of the molecular weight data is not possible.

Another factor that must be considered in evaluating the number-average molecular weight of poly(butyl acrylate) by GPC is the effect of long-chain branching. Butyl acrylate is known to undergo significant chain transfer to polymer, particularly at elevated temperatures and low monomer concentrations.[25−29] Intramolecular chain transfer, or backbiting, causes short-chain branching that has a minimal effect on the hydrodynamic diameter of the polymer, and hence the evaluation of molecular weight by GPC. However, intermolecular chain transfer causes long-chain branching, which can have a significant effect on the hydrodynamic diameter of the polymer. Recent work by Castignolles et al.[29] has confirmed that intramolecular chain transfer dominates in butyl acrylate polymerizations. Roos and Muller reached a similar conclusion in their investigations of controlled butyl acrylate polymerizations using atom transfer radical polymerization.[30] Therefore, the effect of long-chain branching is not considered to be important in the evaluation of the molecular weight data presented below.

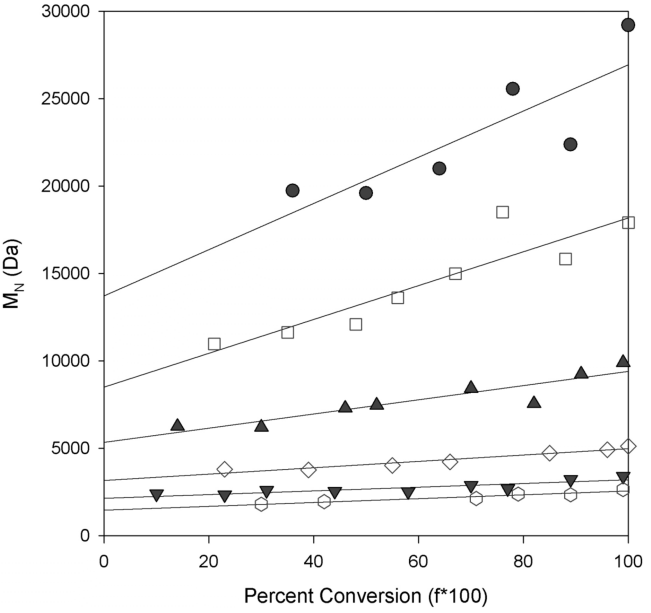

Figure 2. M_N of poly(butyl acrylate) at MOEP/micelle ratios of (●) 0.3, (□) 0.6, (▲) 1.2, (◇) 2.4, (▼) 3.7, and (⬡) 4.9. The lines are least-squares linear fits to the data.

In a controlled polymerization when the concentration of the chain transfer agent is much greater than the initiator concentration, as is true for all of the chain transfer agent per micelle ratios investigated, the number-average molecular weight (M_N) is expected to increase linearly as a function of conversion, i.e.

$$M_N = \frac{MW_{monomer} \cdot [monomer]_0 \cdot conversion}{[CTA]_0} \quad (1)$$

where $MW_{monomer}$ is the molecular weight of the monomer and $[monomer]_0$ and $[CTA]_0$ are the initial concentrations of monomer and chain transfer agent in the microemulsion. Experimentally, M_N does grow linearly for the polymerizations with the high water solubility chain transfer agent, MOEP (Figure 2), but the lines fit to the growth of M_n do not pass through the origin, which indicates either an initial period of rapid uncontrolled polymerization or slow activation of the MOEP.

An initial period of rapid uncontrolled growth is an unlikely source of the deviation of the M_N from the origin because all of the polymers are significantly smaller than would be expected for an uncontrolled microemulsion polymerization. In an uncontrolled microemulsion polymerization the very low concentration of polymers formed by decomposition of the initiator produces polymers with M_N of $\sim 10^6$ Da. A more likely source of this deviation is slow activation of the MOEP due to the partitioning of MOEP between micelles and polymer particles. Small-angle neutron

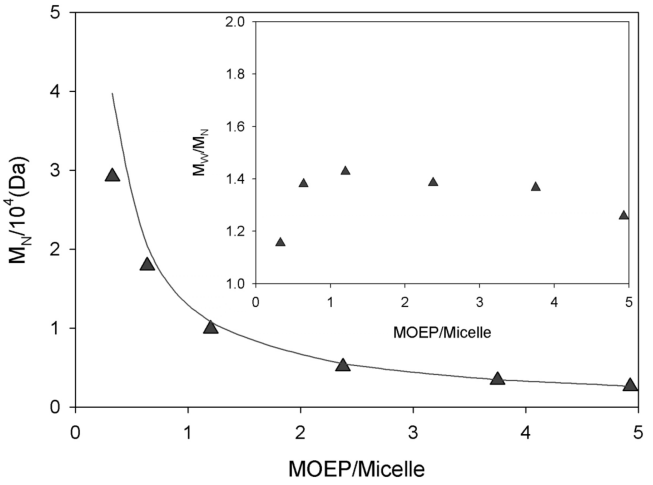

Figure 3. M_N and M_w/M_N (inset) of poly(butyl acrylate) as a function of MOEP/micelle. The line is the predicted final M_N (eq 1 with conversion = 1).

scattering studies have shown that the chain transfer agent remains partitioned between the micelles and polymer particles throughout the polymerization.[31] This partitioning means that at low conversions the concentration of polymers is significantly less than the initial concentration of chain transfer agent in the microemulsion. Therefore, $[CTA]_0$ in eq 1 should to be replaced by the fraction of the chain transfer agent that has been activated as a function of conversion, which results in a much larger M_N than anticipated using eq 1:

$$M_N = \frac{MW_{monomer} \cdot [monomer]_0 \cdot conversion}{\text{fraction activated CTA} \cdot [CTA]_0} \qquad (2)$$

Equation 2 can be used to approximate the fraction of the chain transfer agent that has been activated at a given conversion from the M_N calculated by the least-squares linear fits to the molecular weight data (Figure 2). For example, at 5% conversion the concentration of polymers calculated from the least-squares linear fits to M_N for each of the MOEP/micelle ratios corresponds to only 7−10% of the initial MOEP concentration. As the polymerization proceeds, the MOEP diffuses from the uninitiated micelles into the polymer particles, eventually resulting in activation of all of the chain transfer agent.

The agreement between the measured and predicted final M_N (Figure 3, eq 1 with conversion = 1) indicates that the final concentration of polymer does in fact correspond to the initial concentration of MOEP in the microemulsion, which means that all of the MOEP is activated during the polymerization. Because the number of micelles is ∼1000 times greater than the number of polymer particles, activation of all of the MOEP signifies that MOEP is in fact diffusing into the polymer particles. The diffusion of MOEP into the polymer particles during the polymerization is advantageous for achieving the desired M_N; however, this diffusion causes a broad distribution of the MOEP/particle ratio to develop. This distribution of the MOEP/particle ratio causes the polydispersity (M_W/M_N) of the polymers (Figure 3, inset) to increase as the concentration of MOEP increases for MOEP/micelle ratios less than one. For MOEP/micelle ratios greater than one M_W/M_N decreases slightly, suggesting that the reaction conditions within the polymer particles are more uniform at high MOEP/micelle ratios.

The RAFT microemulsion polymerizations of BA with MODP, the low water solubility chain transfer agent, demonstrate several distinct populations of polymer at all of

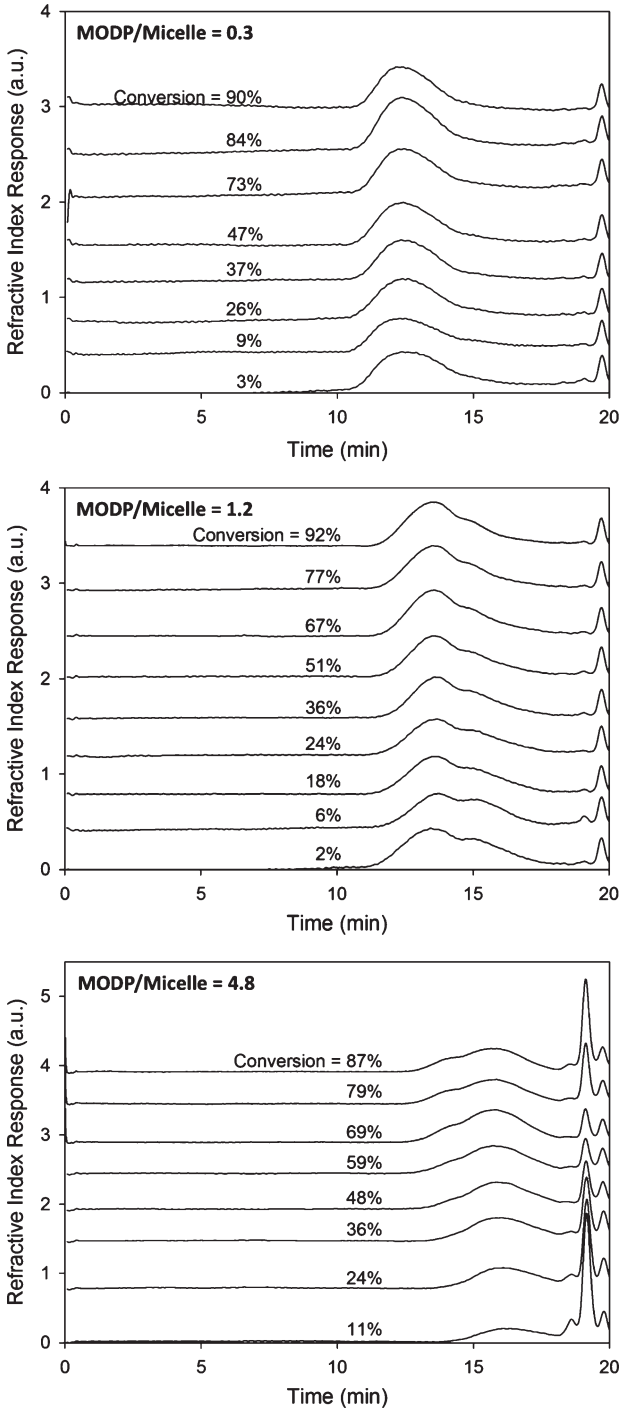

Figure 4. Gel permeation chromatography traces of poly(butyl acrylate) with, from top to bottom, MODP/micelle = 0.3, 1.2, and 4.8. The small refractive index peak that appears at ∼19 min in each plot is a solvent peak.

the MODP/micelle ratios investigated (Figure 4). As with the polymerizations with MOEP, all of the polymers are smaller than those produced by uncontrolled polymerization ($M_N \sim 10^6$ Da), indicating that the polymerization is controlled. At MODP/micelle ratios of 0.3 and 0.6, the gel permeation chromatography (GPC) traces show predominantly 40−60 kDa polymers with a low molecular weight tail. At an MODP/micelle ratio of 1.2, the concentration of low molecular weight polymers increases and two distinct peaks are observed in the GPC trace. The high molecular weight polymers are now 30−50 kDa, and the low molecular

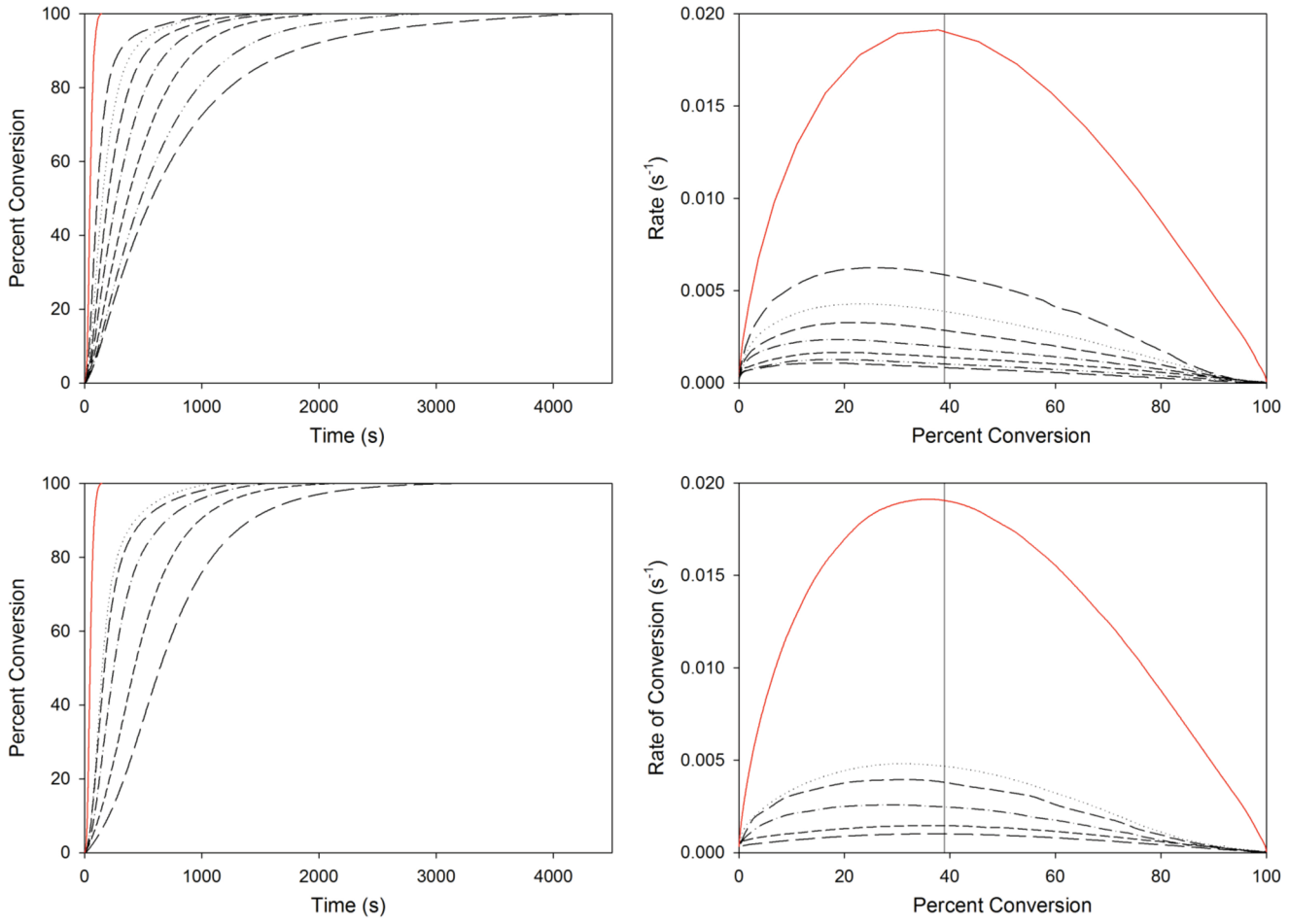

Figure 5. Percent conversion (left) and rate of conversion (right) measured by calorimetry for (top) MOEP/micelle = 0, 0.1, 0.3, 0.6, 1.2, 2.4, 3.7, and 4.9 and (bottom) MODP/micelle = 0, 0.3, 0.6, 1.2, 2.4, and 4.9.

weight polymers are less than 10 kDa. As the MODP/micelle ratio increases from 1.2 to 4.8, the ratio of the high molecular weight polymer to low molecular weight polymer decreases. Additionally, a large concentration of oligomers is apparent in the GPC traces. The appearance of discrete polymer populations in the BA RAFT microemulsion polymerizations with MODP is a direct result of the slow diffusion of the chain transfer agent to the polymer particles. This results in a low chain transfer agent per particle ratio, as discussed further in the following section after examining the polymerization kinetics.

Polymerization Kinetics. All of the BA RAFT microemulsion polymerizations reached 100% conversion, however, as the chain transfer agent per micelle ratio increased the time necessary to reach complete conversion increased significantly (Figure 5). For example, the uncontrolled polymerization of BA was completed within 2 min, while polymerization at an MOEP/micelle ratio of 4.9 required 70 min to reach completion. The increase in polymerization time as the chain transfer agent per micelle ratio increases results solely from rate retardation (Figure 5); no inhibition period was observed. As discussed in more detail in the Kinetic Model section, the increase in rate retardation as the MOEP/micelle ratio increases is a direct result of a dramatic increase in the concentration of dormant polymers in the polymer particles due to diffusion of the CTA from uninitiated micelles to polymer particles. Similar compartmentalization effects on the rate of polymerization have been observed in RAFT (mini)emulsion polymerizations[5,6] as well as in controlled emulsion polymerizations using ATRP[8−11] and NMP.[12−17]

In addition to the decreased rate of polymerization, the percent conversion where the polymerization reaches the rate maximum for the polymerizations with MOEP shifts from 39% conversion, the anticipated rate maximum for an uncontrolled microemulsion polymerization,[32] to lower conversions (Figure 6). In an uncontrolled microemulsion polymerization a shift of the rate maximum to conversions less than 39% signifies either nonlinear monomer partitioning or non-negligible biradical termination reactions.[33] Small-angle neutron scattering experiments have confirmed linear monomer partitioning for all MOEP per micelle ratios investigated.[31] Additionally, the rate maximum for the uncontrolled microemulsion polymerization of BA occurs at 34% conversion, which indicates only a slight effect of biradical termination reactions. Therefore, the shift of the location of the rate maximum as a function of the chain transfer agent per micelle ratio is directly related to the RAFT reaction. The polymerizations with the low water solubility chain transfer agent, MODP, do not show the same shift of the location of the rate maximum as the MOEP polymerizations. In all of the MODP polymerizations the rate maximum occurs at conversions greater than 30%. Kinetic modeling based on the reaction scheme presented in the following section shows that the difference in the location of the rate maximum is directly related to the rate of diffusion of the chain transfer agent.[21] As the rate of chain transfer agent diffusion increases, the activation of the chain

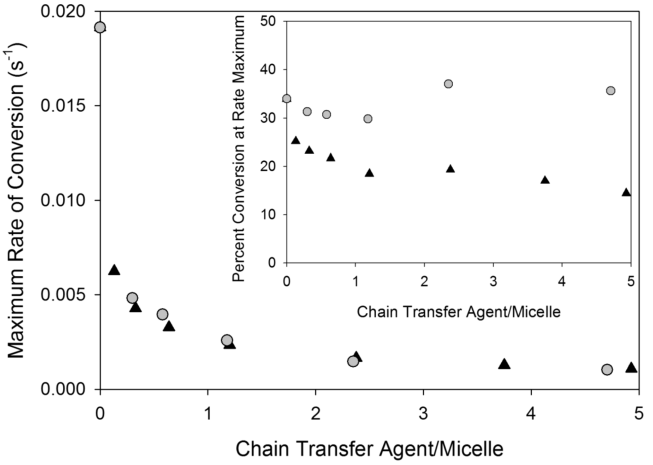

Figure 6. Maximum rate of conversion and percent conversion at the rate maximum (inset) as a function of chain transfer agent/micelle for (▲) MOEP and (●) MODP.

transfer agent shifts from a diffusion-limited to a reaction-limited reaction, causing an increase in the average number of chain transfer agents per particle. This increase in the average number of chain transfer agents per particle enhances rate retardation, which increases the total polymerization time, and thus the concentration of polymer particles formed due to the continual thermal decomposition of the initiator. The probability of a radical entering a polymer particle and causing termination as opposed to entering a micelle and forming a new polymer particle becomes significant as the particle concentration increases, so biradical termination effects are enhanced and the maximum rate of conversion shifts to lower monomer conversions, as shown by de Vries et al.[33]

Kinetic Model. Although the rate maximum appears inversely proportional to the chain transfer agent per micelle ratio (and does not depend on water solubility, Figure 6), the polymerization rate depends on the conditions within each particle, and therefore, the chain transfer agent per *particle* ratio is expected to determine the kinetics. The chain transfer agent per particle ratio is a function of both the initial chain transfer agent per micelle ratio and the rate of diffusion of the chain transfer agent from the micelles to the polymer particles.

The dependence of the location of the rate maximum and the polymer molecular weight distributions on the chain transfer agent per particle ratio can be explained by examining the concentration of propagating polymers ($P^\bullet$) using the proposed RAFT mechanism (Figure 1) and zero-one kinetics. A summary of this kinetic model is provided here, and complete details of the model development and results are published elsewhere.[34] Three types of reactions occur within each polymer particle: propagation, activation of the chain transfer agent, and exchange between active and dormant polymers. Propagation does not affect the concentration of $P^\bullet$ in the particle and need not be considered further. The simplified chain transfer agent activation reaction is given by

$$P\bullet + XR \rightarrow XP + R\bullet$$

where XR is the chain transfer agent, XP is the dormant polymer, and $R^\bullet$ is the leaving group of the chain transfer agent. The reinitiation reaction

$$R\bullet + M \rightarrow P\bullet$$

where M is the monomer, can be combined with the simplified chain transfer agent activation reaction by noting that the rate of reinitiation[35] ($k_i \sim 1000$ L mol^{-1} s^{-1}) is rapid relative to the rate of transfer[36] ($k_{tr} \sim 100$ L mol^{-1} s^{-1}), which gives the net reaction

$$P\bullet + XR \rightarrow XP + P\bullet$$

This combined activation and reinitiation equation also does not change the concentration of $P^\bullet$.

The concentration of propagating radicals in the particle [$P^\bullet$] then depends only on the exchange between active and dormant polymers

$$P\bullet + XP \leftrightarrow PX\bullet P$$

and the rate equation for [P•] becomes

$$\frac{d[P^\bullet]}{dt} = \frac{-k_a}{N_A V_{part}}[XP][P^\bullet] + 2k_f[PX^\bullet P]$$

where [XP] is the concentration of dormant polymers per particle, [$PX^\bullet P$] is the concentration of macroRAFT radicals per particle, k_a is the addition rate constant, k_f is the fragmentation rate constant, N_A is Avogadro's number, and V_{part} is the volume of a single particle. All concentrations are in units of molecules per particle. In a microemulsion polymerization, the assumption of zero-one kinetics is valid because the number of micelles is ~1000 times greater than the number of polymer particles, so the probability of a second radical entering a polymer particle is negligible. Therefore, each particle contains either a single $P^\bullet$ without any $PX^\bullet P$ or a single $PX^\bullet P$ without a $P^\bullet$. The rate equation for [$P^\bullet$] in an active particle (for which [$P^\bullet$] = 1 and [$PX^\bullet P$] = 0) is then

$$\left(\frac{d[P^\bullet]}{dt}\right)_{active} = \frac{-k_a}{N_A V_{part}}[XP] \quad (3)$$

The rate equation for [$P^\bullet$] in a dormant particle is

$$\left(\frac{d[P^\bullet]}{dt}\right)_{dormant} = 2k_f \quad (4)$$

Equation 4 implies that the time a particle remains dormant is inversely proportional to the fragmentation rate constant:

$$t_{dormant} = \frac{1}{2k_f} \quad (5)$$

To solve eq 3 for the time that a particle remains active, [XP] and V_{part} must be known as a function of reaction time. However, [XP] depends on both [XR] at the time the propagating oligomeric radical enters the particle and the diffusion of XR into the particle between the time the oligomeric radical enters and all later times, as shown by Hermanson and Kaler.[37] The dependence of [XP] on both the reaction time and the particle initiation time and the coupling of the rate of diffusion of XR with the fraction of particles that are active prevent the development of a simple closed expression for [XP].

However, the average time that a particle remains active can be estimated by assuming that chain transfer agent diffuses into the propagating particles slowly throughout the polymerization, as opposed to rapidly partitioning into the particles during the early stages of the polymerization. This assumption is supported by both small-angle neutron scattering (SANS) studies of monomer partitioning in these RAFT microemulsion polymerizations,[31] and the observed

reaction kinetics. SANS was used to monitor the microstructural evolution of the monomer and chain transfer agent swollen micelles and polymer particles as a function of conversion. The micelles continuously decrease in size as a function of conversion, which confirms that the monomer remains partitioned between the polymer particles and the micelles throughout the polymerization. This is also the case for uncontrolled microemulsion polymerizations.[19,38] The MOEP and MODP are expected to remain partitioned between the polymer particles and micelles as well because the aqueous solubilities of MOEP (1.0 mM) and MODP (< 0.01 mM) are less than that of BA (10.9 mM). Additionally, if the chain transfer agent were consumed early in the polymerization, the rate of reaction should increase at higher conversions due to the uncontrolled polymerization of newly initiated polymer particles, and this is not observed in the polymerization kinetics.

Assuming that chain transfer agent diffuses slowly into the polymer particles means that [XP] is approximately constant over the time that a particle remains active. Similarly, the increase in particle size over the time that a particle remains active can be assumed negligible, so V_{part} is constant. The characteristic time that a particle remains active is inversely proportional to [XP]:

$$t_{active} \approx \frac{1}{\frac{k_a}{N_A V_{part}}[XP]} \tag{6}$$

For a large number of polymer particles the system is ergodic, so combining eqs 5 and 6 the fraction of initiated polymer radicals that remain active (x_{act}) is inversely proportional to [XP]:

$$X_{act} = \frac{t_{active}}{t_{active} + t_{dormant}} = \frac{1}{\frac{k_a}{2k_f N_A V_{part}}[XP] + 1} \tag{7}$$

This result shows that the diffusion of chain transfer agent into the polymer particles critically impacts the polymerization kinetics by significantly increasing [XP] and consequently decreasing the concentration of propagating radicals.

Model M_N Distribution. The kinetic model developed in the previous section can be used to examine the trends of the M_N distribution caused by the chain transfer agent solubility. This model shows that although multimodal molecular weight distributions are expected for all RAFT microemulsion polymerizations, the distinct populations of polymer molecular weights are indistinguishable by techniques such as gel permeation chromatography.

The number-average molecular weight of the polymers *in a given particle* ($M_{N,part}$) depends on both the amount of monomer consumed by the particle and the number of chain transfer agents in the particle. The average amount of monomer that is consumed by a polymer particle during a RAFT microemulsion polymerization (M_{part}) is proportional to the fraction of time that a particle is in the active state. So, from eq 7

$$M_{part}([XP]) \propto x_{act} = \frac{1}{\frac{k_a}{2k_f N_A V_{part}}[XP] + 1} \tag{8}$$

Equation 8 shows that particles with a high [XP] (a large amount of dormant polymer) consume less monomer over the course of the polymerization than particles with a low [XP].

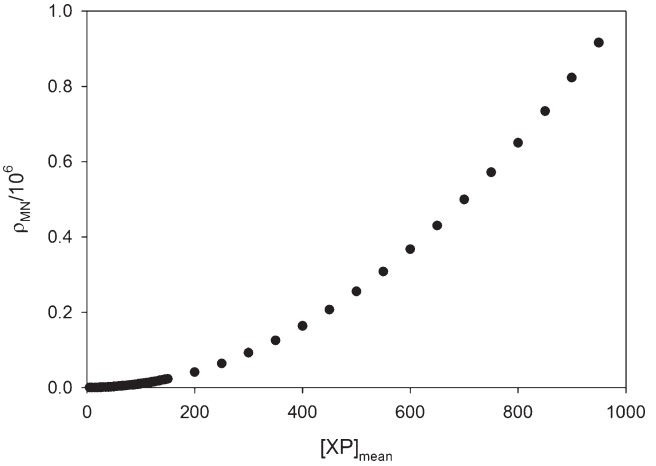

Figure 7. M_N population density as a function of $[XP]_{mean}$ calculated from eq 13 with $k_a = 10^5\ M^{-1}\ s^{-1}$, $k_f = 10^{-2}\ s^{-1}$, and $V_{part} = 4.2 \times 10^3\ nm^3$. Note that adjusting the values of the rate constant k_f within the range of values reported in the literature (10^{-6}–$10^2\ s^{-1}$)[39,40] alters the absolute magnitude of ρ_{MN}, but not the relative increases in ρ_{MN} with $[XP]_{mean}$.

The monomer consumed by a particle during the polymerization is distributed among the polymer chains within the particle or equivalently the number of dormant polymers in the particle, [XP]. To determine the average M_N in a particle ($M_{N,part}$), the amount of monomer consumed by the particle (M_{part}, eq 8) is divided by the number of dormant polymers in the particle [XP] to give

$$M_{N,part}([XP]) \propto \frac{1}{[XP]}\left(\frac{1}{\frac{k_a}{2k_f N_A V_{part}}[XP] + 1}\right) \tag{9}$$

Equation 9 predicts that $M_{N,part}$ decreases as the concentration of dormant polymers ([XP]) increases, which is consistent with the trend predicted for the overall M_N in a RAFT polymerization given by eq 2. The expression for $M_{N,part}$ in a particle containing [XP] chain transfer agents, given by eq 9, can now be used to examine the effect of chain transfer agent diffusion on the experimentally observed M_N distribution, as measured by GPC.

A distribution of the chain transfer agent among the particles must be assumed to examine the effects of chain transfer agent diffusion on the M_N distribution. A Poisson distribution of the chain transfer agent among the polymer particles with a mean value of dormant polymers ([XP]) in a particle given by $[XP]_{mean}$ has been selected for the following mathematical description of the M_N distribution. For concreteness, the M_N distribution presented here considers only the population of particles containing a number of chain transfer agents within one standard deviation of $[XP]_{mean}$, where the standard deviation (σ) of the Poisson distribution is related to the mean (μ) by

$$\sigma = \sqrt{\mu} \tag{10}$$

The concentration of polymer particles containing a number of chain transfer agents outside of one standard deviation of the mean is negligibly small. For a Poisson distribution, the number of population elements (N) within one standard deviation (σ) of the mean (μ) is

$$N = 2\sqrt{\mu} + 1 \tag{11}$$

So, the number of discrete chain transfer agent per particle ratios contained within the population of interest (N_{pop})

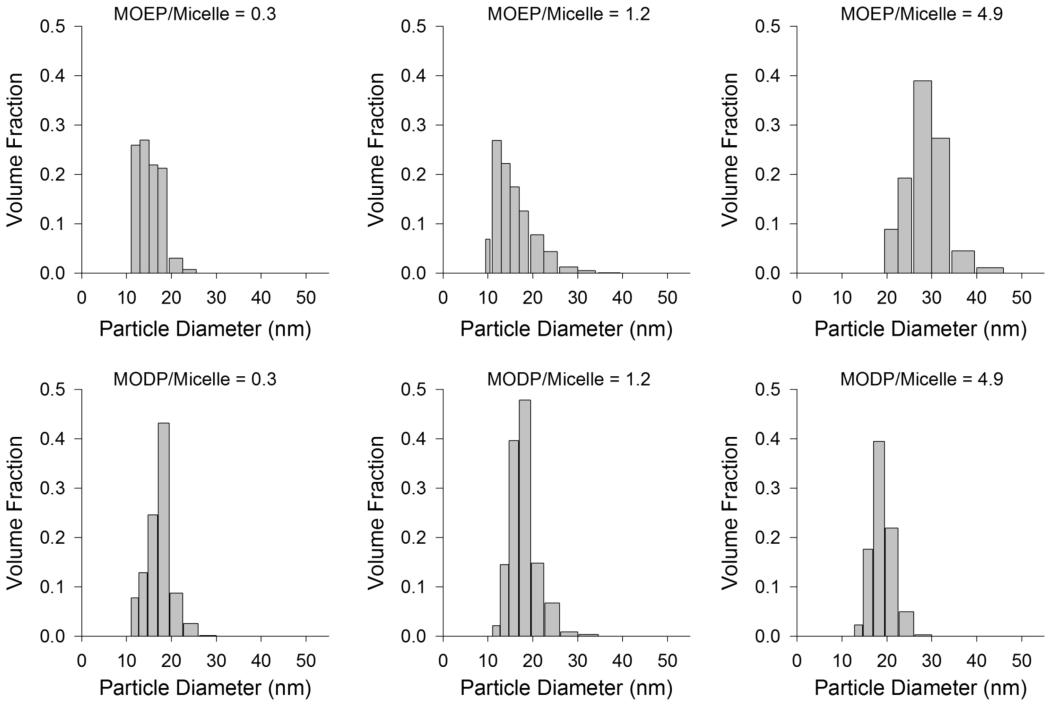

Figure 8. Average of four CONTIN fits to quasi-elastic light scattering data for poly(butyl acrylate) latex particles polymerized with MOEP (top) or MODP (bottom) at chain transfer agent/micelle ratios of 0.3, 1.2, and 4.9.

is then

$$N_{pop} = 2\sqrt{[XP]_{mean}} + 1 \quad (12)$$

Each chain transfer agent per particle ratio corresponds to a single $M_{N,part}$, as shown by eq 9, so N_{pop} is also equal to the number of discrete molecular weight populations that are produced by the particles within the [XP] population of interest ($[XP]_{mean} \pm \sigma$). The ability to detect these discrete molecular weight populations by experimental techniques such as GPC depends on the number of molecular weight populations (N_{pop}) contained within the total range of molecular weights ($M_{N,part}([XP]_{mean} \pm \sigma)$), which can be defined as a density of M_N populations (ρ_{MN})

$$\rho_{MN} = \frac{N_{pop}}{M_{N,part}([XP]_{mean} - \sigma) - M_{N,part}([XP]_{mean} + \sigma)} \quad (13)$$

Figure 7 shows that ρ_{MN} increases dramatically as $[XP]_{mean}$ increases. Thus, the high $[XP]_{mean}$ in the MOEP polymerizations, caused by the rapid diffusion of this high water solubility chain transfer agent into the particles, leads to one broad peak in the GPC trace. On the other hand, the low water solubility chain transfer agent, MODP, maintains a low $[XP]_{mean}$, so ρ_{MN} is low and the discrete M_N populations are observed in the GPC traces (Figure 4).

Latex Particle Size. The latex particle size distribution (Figure 8) also depends on the distribution of chain transfer agent in the polymer particles. The uncontrolled microemulsion polymerization of BA produces latex particles with a very narrow distribution of diameters between 35 and 45 nm. The addition of the chain transfer agent at chain transfer agent per micelle ratios of only 0.3 drastically reduces the latex particle diameter, but the distribution is still narrow. As the MOEP/micelle ratio increases beyond 0.3, the particle size distribution broadens and the average latex particle diameter increases. The initial decrease and subsequent increase in the average latex particle diameter as the MOEP/micelle ratio increases is directly related to the rate retardation. The increased polymerization time both increases the number of polymer particles formed by thermal decomposition of the initiator, resulting in smaller particles, and facilitates coalescence of the monomer swollen polymer particles, thereby increasing the size of some of the particles. Both events contribute to the broader distribution. Increasing the MODP/micelle ratio does not cause an increase in the latex particle diameter, indicating that coalescence is less likely in the polymerizations with the low solubility chain transfer agent.

Conclusions

The rate of diffusion of chain transfer agent from uninitiated micelles into propagating polymer particles is a key parameter for determining the properties of the polymer and latex produced by RAFT microemulsion polymerizations. RAFT microemulsion polymerizations of BA with MOEP, a high water solubility chain transfer agent, produced stable latex nanoparticles (20−30 nm in diameter) containing low polydispersity polyBA of predetermined molecular weight. However, polymerizations with MODP, a low water solubility chain transfer agent, produced stable latex nanoparticles containing polymers with a multimodal molecular weight distribution. The differences between these polymerizations correspond to kinetic and molecular weight trends predicted from calculations of the fraction of time that a particle is in the active state, which is inversely proportional to the concentration of the chain transfer agent in the particles.

References and Notes

(1) Chiefari, J.; Chong, Y. K.; Ercole, F.; Krstina, J.; Jeffery, J.; Le, T. P. T.; Mayadunne, R. T. A.; Meijs, G. F.; Moad, C. L.; Moad, G.; Rizzardo, E.; Thang, S. H. Living free-radical polymerization by reversible addition-fragmentation chain transfer: The RAFT process. *Macromolecules* **1998**, *31* (16), 5559–5562.

(2) Moad, G.; Chiefari, J.; Chong, Y. K.; Krstina, J.; Mayadunne, R. T. A.; Postma, A.; Rizzardo, E.; Thang, S. H. Living free radical polymerization with reversible addition-fragmentation chain transfer (the life of RAFT). *Polym. Int.* **2000**, *49* (9), 993–1001.

(3) Rizzardo, E.; Chiefari, J.; Mayadunne, R.; Moad, G.; Thang, S. Tailored polymer architectures by reversible addition-fragmentation chain transfer. *Macromol. Symp.* **2001**, *174*, 209–212.
(4) Prescott, S. W.; Ballard, M. J.; Rizzardo, E.; Gilbert, R. G. RAFT in emulsion polymerization: What makes it different? *Aust. J. Chem.* **2002**, *55* (6−7), 415–424.
(5) Cunningham, M. F. Controlled/living radical polymerization in aqueous dispersed systems. *Prog. Polym. Sci.* **2008**, *33* (4), 365–398.
(6) Luo, Y. W.; Wang, R.; Yang, L.; Yu, B.; Li, B. G.; Zhu, S. P. Effect of reversible addition-fragmentation transfer (RAFT) reactions on (mini)emulsion polymerization kinetics and estimate of RAFT equilibrium constant. *Macromolecules* **2006**, *39* (4), 1328–1337.
(7) Lansalot, M.; Davis, T. P.; Heuts, J. P. A. RAFT miniemulsion polymerization: Influence of the structure of the RAFT agent. *Macromolecules* **2002**, *35* (20), 7582–7591.
(8) Simms, R. W.; Cunningham, M. F. Compartmentalization of reverse atom transfer radical polymerization in miniemulsion. *Macromolecules* **2008**, *41* (14), 5148–5155.
(9) Kagawa, Y.; Kawasaki, M.; Zetterlund, P. B.; Minami, H.; Okubo, M. Atom transfer radical polymerization of iso-butyl methacrylate in microemulsion with cationic and non-ionic emulsifiers. *Macromol. Rapid Commun.* **2007**, *28* (24), 2354–2360.
(10) Kagawa, Y.; Zetterlund, P. B.; Minami, H.; Okubo, M. Atom transfer radical polymerization in miniemulsion: Partitioning effects of copper(I) and copper(II) on polymerization rate, livingness, and molecular weight distribution. *Macromolecules* **2007**, *40* (9), 3062–3069.
(11) Kagawa, Y.; Zetterlund, P. B.; Minami, H.; Okubo, M. Compartmentalization in atom transfer radical polymerization (ATRP) in dispersed systems. *Macromol. Theory Simul.* **2006**, *15* (8), 608–613.
(12) Cunningham, M. F. Recent progress in nitroxide-mediated polymerizations in miniemulsion. *C. R. Chim.* **2003**, *6* (11−12), 1351–1374.
(13) Zetterlund, P. B.; Okubo, M. Compartmentalization in NMP in Dispersed Systems: Relative Contributions of Confined Space Effect and Segregation Effect Depending on Nitroxide Type. *Macromol. Theory Simul.* **2009**, *18* (4−5), 277–286.
(14) Zetterlund, P. B.; Kagawa, Y.; Okubo, M. Compartmentalization in Atom Transfer Radical Polymerization of Styrene in Dispersed Systems: Effects of Target Molecular Weight and Halide End Group. *Macromolecules* **2009**, *42* (7), 2488–2496.
(15) Wakamatsu, J.; Kawasaki, M.; Zetterlund, P. B.; Okubo, M. Nitroxide-mediated radical polymerization in microemulsion. *Macromol. Rapid Commun.* **2007**, *28* (24), 2346–2353.
(16) Zetterlund, P. B.; Wakamatsu, J.; Okubo, M. Nitroxide-Mediated Radical Polymerization of Styrene in Aqueous Microemulsion: Initiator Efficiency, Compartmentalization, and Nitroxide Phase Transfer. *Macromolecules* **2009**, *42* (18), 6944–6952.
(17) Nicolas, J.; Charleux, B.; Magnet, S. Multistep and semibatch nitroxide-mediated controlled free-radical emulsion polymerization: A significant step toward conceivable industrial processes. *J. Polym. Sci., Part A: Polym. Chem.* **2006**, *44* (13), 4142–4153.
(18) Liu, S.; Hermanson, K. D.; Kaler, E. W. Reversible addition-fragmentation chain transfer polymerization in microemulsion. *Macromolecules* **2006**, *39* (13), 4345–4350.
(19) Co, C. C.; de Vries, R.; Kaler, E. W. Microemulsion polymerization. 1. Small-angle neutron scattering study of monomer partitioning. *Macromolecules* **2001**, *34* (10), 3224–3232.
(20) van Os, N. M. *Physico-chemical Properties of Selected Anionic, Cationic, and Nonionic Surfactants*; Elsevier: Amsterdam, 1993.
(21) O'Donnell, J. Reversible Addition-Fragmentation Chain Transfer Polymerization in Microemulsions. Ph.D. Thesis, Chemical Engineering, University of Delaware, **2007**.
(22) Hutchinson, R. A.; McMinn, J. H.; Paquet, D. A.; Beuermann, S.; Jackson, C. A pulsed-laser study of penultimate copolymerization propagation kinetics for methyl methacrylate n-butyl acrylate. *Ind. Eng. Chem. Res.* **1997**, *36* (4), 1103–1113.
(23) Beuermann, S.; Paquet, D. A.; McMinn, J. H.; Hutchinson, R. A. Determination of free-radical propagation rate coefficients of butyl, 2-ethylhexyl, and dodecyl acrylates by pulsed-laser polymerization. *Macromolecules* **1996**, *29* (12), 4206–4215.
(24) Guillaneuf, Y.; Castignolles, P. Using apparent molecular weight from SEC in controlled/living polymerization and kinetics of polymerization. *J. Polym. Sci., Part A: Polym. Chem.* **2008**, *46* (3), 897–911.
(25) Arzamendi, G.; Plessis, C.; Leiza, J. R.; Asua, J. M. Effect of the intramolecular chain transfer to polymer on PLP/SEC experiments of alkyl acrylates. *Macromol. Theory Simul.* **2003**, *12* (5), 315–324.
(26) Plessis, C.; Arzamendi, G.; Alberdi, J. M.; van Herk, A. M.; Leiza, J. R.; Asua, J. M. Evidence of branching in poly(butyl acrylate) produced in pulsed-laser polymerization experiments. *Macromol. Rapid Commun.* **2003**, *24* (2), 173–177.
(27) Plessis, C.; Arzamendi, G.; Leiza, J. R.; Schoonbrood, H. A. S.; Charmot, D.; Asua, J. M. Seeded semibatch emulsion polymerization of n-butyl acrylate. Kinetics and structural properties. *Macromolecules* **2000**, *33* (14), 5041–5047.
(28) Plessis, C.; Arzamendi, G.; Leiza, J. R.; Schoonbrood, H. A. S.; Charmot, D.; Asua, J. M. Modeling of seeded semibatch emulsion polymerization of n-BA. *Ind. Eng. Chem. Res.* **2001**, *40* (18), 3883–3894.
(29) Castignolles, P.; Graf, R.; Parkinson, M.; Wilhelm, M.; Gaborieau, M. Detection and quantification of branching in polyacrylates by size-exclusion chromatography (SEC) and melt-state C-13 NMR spectroscopy. *Polymer* **2009**, *50* (11), 2373–2383.
(30) Roos, S. G.; Muller, A. H. E. Evidence for chain transfer in the atom transfer radical polymerization of butyl acrylate. *Macromol. Rapid Commun.* **2000**, *21* (12), 864–867.
(31) O'Donnell, J.; Kaler, E. W. Microstructure evolution and monomer partitioning in reversible addition-fragmentation chain transfer microemulsion polymerization. *Macromolecules* **2008**, *41* (16), 6094–6099.
(32) Morgan, J. D.; Lusvardi, K. M.; Kaler, E. W. Kinetics and mechanism of microemulsion polymerization of hexyl methacrylate. *Macromolecules* **1997**, *30* (7), 1897–1905.
(33) de Vries, R.; Co, C. C.; Kaler, E. W. Microemulsion polymerization. 2. Influence of monomer partitioning, termination, and diffusion limitations on polymerization kinetics. *Macromolecules* **2001**, *34* (10), 3233–3244.
(34) O'Donnell, J.; Kaler, E. W. Model of Reversible Addition-Fragmentation Chain Transfer Polymerization in Microemulsions. *J. Polym. Sci., Part A: Polym. Chem.* **2010**, *48* (3), 604−613.
(35) Berger, K. C.; Meyerhoff, G. Propagation and Termination Constants in Free Radical Polymerization. In *Polymer Handbook*; Brandup, J., Immergut, E. H., Eds.; Wiley-Interscience: New York, 1989.
(36) Adamy, M.; van Herk, A. M.; Destarac, M.; Monteiro, M. J. Influence of the chemical structure of MADIX agents on the RAFT polymerization of styrene. *Macromolecules* **2003**, *36* (7), 2293–2301.
(37) Hermanson, K. D.; Liu, S.; Kaler, E. W. Kinetic modeling of controlled living microemulsion polymerizations that use reversible addition-fragmentation chain transfer. *J. Polym. Sci., Part A: Polym. Chem.* **2006**, *44* (20), 6055–6070.
(38) Co, C. C.; Kaler, E. W. Particle size and monomer partitioning in microemulsion polymerization. 2. Online small angle neutron scattering studies. *Macromolecules* **1998**, *31* (10), 3203–3210.
(39) Barner-Kowollik, C.; Quinn, J. F.; Morsley, D. R.; Davis, T. P. Modeling the reversible addition-fragmentation chain transfer process in cumyl dithiobenzoate-mediated styrene homopolymerizations: Assessing rate coefficients for the addition-fragmentation equilibrium. *J. Polym. Sci., Part A: Polym. Chem.* **2001**, *39* (9), 1353–1365.
(40) Wang, A. R.; Zhu, S. P. Modeling the reversible addition-fragmentation transfer polymerization process. *J. Polym. Sci., Part A: Polym. Chem.* **2003**, *41* (11), 1553–1566.